Polymer/Carbon Nanotube Nanocomposites via Noncovalent Grafting with End-Functionalized Polymers

Sun Hwa Lee, Ji Sun Park, Bo Kyung Lim, Sang Ouk Kim

Department of Materials Science and Engineering, Institute for the Nanocentury, Korea Advanced Institute of Science and Technology, Daejeon 305-701, Republic of Korea

Received 21 October 2007; accepted 2 December 2007
DOI 10.1002/app.27920
Published online 18 August 2008 in Wiley InterScience (www.interscience.wiley.com).

ABSTRACT: Polymer/carbon nanotube nanocomposites were fabricated with end-functionalized polymers as dispersants. End-functionalized polymers having amine or carboxylic acid were noncovalently grafted to multiwalled nanotubes (MWNTs). The functional groups of the polymers interacted with the defect sites of purified MWNTs through zwitterionic interactions or hydrogen bonding. This approach provided both an improved dispersion state of MWNTs in an organic solution and polymer matrix and good interfacial adhesion between MWNTs and a matrix. Physical properties, such as the electrical resistivity and mechanical strength, of polystyrene/MWNT nanocomposites were greatly improved through this simple noncovalent functionalization. © 2008 Wiley Periodicals, Inc. J Appl Polym Sci 110: 2345–2351, 2008

Key words: dispersions; functionalization of polymers; nanocomposites

INTRODUCTION

For polymer/carbon nanotube (CNT) nanocomposites, there are still a few issues to be overcome before practical applications. CNTs spontaneously bundle because of the strong van der Waals interaction.[1,2] The bundled CNTs may slip past one another, following the initiated cracks in nanocomposites rather than reinforcing them. The bundling also prevents the building of percolated structures, which is crucial for an effective reinforcement. Another significant issue is the interfacial adhesion with a polymer matrix. This is more critical for CNTs than any other filler because the CNT surfaces are extremely smooth and the interfacial area is huge.[3–5] If a strong polymer/CNT interface could be ensured, the exterior load on the matrix would be efficiently transferred to nanotubes, and nanocomposites with excellent mechanical properties could be accomplished.

To enhance the dispersibility and interfacial adhesion of CNTs in a polymer, a variety of functionalization methods have been developed. Covalent functionalization is a strategy that creates defects on the CNT surface and covalently attaches polymers or any other functional molecules.[6–8] Although the direct linkage between CNTs and a matrix may improve both the dispersion and interfacial adhesion of CNTs, the modification process is complicated and significantly degrades the physical properties of CNTs.[9] Noncovalent functionalization is usually achieved by van der Waals forces or π–π interactions.[9–12] This makes it possible to exclude any significant degradation of the inherent properties of CNTs. However, the applicable solvents and polymers are usually limited because frequently used amphiphilic dispersing agents such as surfactants and biopolymers are generally useful in aqueous media.[11–15] These dispersion agents would remain as impurities after fabrication of the nanocomposites, causing severe degradation of their properties.

Here we demonstrate polymer/CNT nanocomposites relying on a facile and robust noncovalent CNT functionalization method using end-functionalized polymers. Multiwalled nanotubes (MWNTs) were purified by a routinely applied process, which yielded a limited number of carboxyl groups on the cutting edges and surfaces. Various end-functionalized polymers with amine or carboxylic acid groups readily interacted with the defect sites, so the noncovalent grafting of a polymer was accomplished through a simple solution-mixing process. This

Additional Supporting Information may be found in the online version of this article.

Correspondence to: S. O. Kim (sangouk.kim@kaist.ac.kr).

Contract grant sponsor: Brain Korea 21 Project.
Contract grant sponsor: Korea Research Foundation; contract grant number: KRF-2005-003-D00085.
Contract grant sponsor: Basic Research Program of the Korea Science & Engineering Foundation; contract grant number: R01-2005-000-10456-0.
Contract grant sponsor: Korean Ministry of Science and Technology.
Contract grant sponsor: Fundamental R&D Program for Core Technology of Materials (funded by the Ministry of Commerce, Industry, and Energy, Republic of Korea).

remarkably enhanced the interfacial adhesion between CNTs and a matrix polymer as well as the dispersibility of CNTs in organic solvents and a polymer matrix. We fabricated polystyrene (PS)/MWNT nanocomposites with various end-functionalized PSs as dispersants and characterized the reinforcing effect on their electrical, optical, and mechanical properties.

EXPERIMENTAL

Materials

MWNTs were purchased from Iljin Nanotec, Inc. (Seoul, Korea) Benzene was purchased from Merck (Darmstadt, Germany). Monodisperse amine terminated polystyrene (PS–NH_2), carboxylic acid terminated polystyrene (PS–COOH), and PS with the same weight-average molecular weight (M_w) of 3000 g/mol were purchased from Polymer Source, Inc. (Montreal, Canada) PS–COOH with M_w = 50,000 g/mol was purchased from Scientific Polymer Products, Inc. (Ontario, NY) PS with M_w = 50,000 g/mol was purchased from Polysciences, Inc. (Warrington, PA). All materials except MWNTs were used without further purification. MWNTs were purified by sonication in a mixture of sulfuric acid and nitric acid (3 : 1 v/v) for 10 h. The temperature of the acid solution was maintained at about 60–70°C. Upon sonication, the impurities, including metal catalysts, were removed, and a limited number of carboxyl functional groups were formed at the edges and sidewalls of the MWNTs (Table S.I). Amorphous carbon and residual acid solutions were removed by subsequent heat treatment at 400°C, which was continued for 40 min under atmospheric conditions.

Fourier transform Raman (FT-Raman) characterization of MWNT–polymer interactions

The samples for Raman measurements were prepared by the sonication of MWNTs and monodisperse polymers (PS, PS–COOH, or PS–NH_2; M_w = 3000 g/mol) in chloroform. The FT-Raman spectra of the prepared samples were recorded on a Bruker (Billerica, MA) RFS-100 with a 1064-nm laser of 100 mW. The number of scans was 256, and the scanning resolution was 2 cm^{-1}. The concentration of the MWNTs and polymer was 2 and 40 mg/mL, respectively, in all samples, and the solvent background was corrected.

Preparation and characterization of the PS/MWNT nanocomposite films

For the preparation of the nanocomposites, four kinds of matrices were used: PS (M_w = 50,000 g/mol), PS–COOH (M_w = 50,000 g/mol), a mixture of PS–NH_2 (M_w = 3000 g/mol) and PS (M_w = 50,000 g/mol), and a mixture of PS–COOH (M_w = 3000 g/mol) and PS (M_w = 50,000 g/mol). The concentration of end-functionalized polymers in the matrix was 10 wt %. Predetermined amounts of the purified MWNTs (0.2–10 wt % of the matrix polymer) and matrix polymer (5 wt % of the entire solution) were dispersed in benzene by sonication. The prepared dispersion was spin-coated onto a glass or silicon substrate to prepare a nanocomposite film. The morphologies of CNTs in the prepared nanocomposites were examined with a Hitachi S4800 scanning electron microscope (Kyoto, Japan). The scanning electron microscopy (SEM) sample was prepared by the fracturing of a nanocomposite film on a substrate. Weak reactive-ion etching (RIE) was applied at the film surface to reveal the MWNTs inside the polymer matrix. The conditions of RIE were 50 W, 0.06 Torr of O_2, and 20 s. The optical transparency of a nanocomposite film coated on a slide glass was characterized by ultraviolet–visible spectroscopy with a Shimadzu UV-3101PC. The transmittance of visible light was scanned for wavelengths ranging from 400 to 800 nm. A bare slide glass without film was used as a reference. The electrical conductivity of a nanocomposite film was measured with a four-point probe (CMT-SR 1000, Changmin Co., Seongnam, Korea). The mechanical properties were measured with nanoindentation (XP, MTS, Eden Prairie, MN).

RESULTS AND DISCUSSION

The noncovalent interaction between MWNTs and end-functionalized polymers was simply demonstrated by the model experiment presented in Figure 1. The dark phase at the bottom of each vial corresponds to the aqueous dispersion of MWNTs temporarily stabilized by ultrasonication without any dispersing agent. Because the purified MWNTs possessed polar carboxylic groups at the cutting edge and side wall, they could be temporarily dispersed in aqueous media. The organic phase located over the aqueous phase corresponds to pure benzene, the benzene solution of nonfunctionalized PS, the benzene solution of PS–COOH, or the benzene solution of PS–NH_2, as indicated. All used polymers were monodisperse in their molecular weights and had the same molecular weight of 3000 g/mol. Most of the vials showed a concave meniscus of the oil phase, except that containing the benzene solution of PS–NH_2, which showed a convex meniscus. The segregation of the terminal amine group remarkably reduced the interfacial tension between the oil phase and the glass surface. Notably, despite the presence of the polar carboxylic acid groups, the vial containing PS–COOH showed a concave meniscus. Unlike

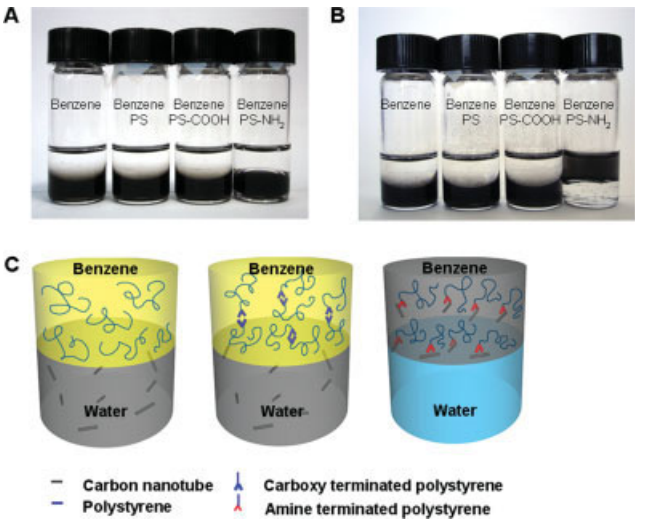

Figure 1 Photographs and a schematic for transferring MWNTs from an aqueous phase to an oil phase by the introduction of an end-functionalized polymer. (A,B) The lower phases are aqueous dispersions of MWNTs, and the upper phases are pure benzene or benzene solutions of PS, PS–COOH, and PS–NH_2: (A) before and (B) after stirring for 24 h. The molecular weight of all three kinds of polymers was 3000 g/mol. (C) Schematic for the noncovalent interaction between MWNTs and polymers. Only the oil phase including PS–NH_2 interacted strongly with MWNTs for extraction from the aqueous phase. [Color figure can be viewed in the online issue, which is available at www.interscience.wiley.com.]

amine groups, carboxylic acid groups couple with one another through hydrogen bonding, which screens the functionality of the terminal groups. After 24 h of stirring, no significant change was evident in the left three vials [Fig. 1(B)]. However, in the vial containing the benzene solution of PS–NH_2, the oil phase became black, whereas the aqueous phase became completely transparent; this indicated that most MWNTs had transferred from the aqueous phase to the benzene phase. As depicted in Figure 1(C), the oil phase containing nonfunctionalized PS or PS–COOH did not interact with CNTs significantly. Only the oil phase including PS–NH_2 interacted strongly enough to attract MWNTs from the aqueous phase. When the concentration was significantly increased, PS–COOH could also disperse the MWNTs (Fig. S.1). At a low concentration of PS–COOH, they coupled with one another without influencing the MWNTs. However, the opportunity for interaction with MWNTs increased with the concentration of PS–COOH. The nonfunctionalized PS could not disperse MWNTs for all concentrations.

The noncovalent interaction between MWNTs and end-functionalized polymers was investigated with an FT-Raman spectroscopic analysis of the PS/MWNT nanocomposites prepared by a simple solution-mixing process. Figure 2 exhibits Raman spectra of the pure MWNTs and PS/MWNT nanocomposites from 1064-nm laser excitation. In all spectra, two bands around 1600 (G band) and 1290 cm^{-1} (D band) appeared. The graphite G band is related to the tangential mode vibration of the sp^2 C atoms, whereas the D band is induced by scattering from disordered sp^3 C atoms.[16] The intensity ratio of the D and G bands for pure MWNTs is remarkably small because of the limited number of defect sites in the as-purified MWNTs. The nonfunctionalized PS/MWNT nanocomposites showed almost the same Raman spectra as pure MWNTs. The intensity of the D band was slightly increased because of the interaction between the benzene ring of PS with the graphite surface, even though the interaction was not sufficient to disperse MWNTs in an organic solvent. By contrast, the D/G band intensity ratios of the hybrids made from PS–COOH or PS–NH_2 markedly increased. This verifies that the defect sites interacted sensitively with the end groups of the functionalized PS. The slight upshifts of the G band of the hybrids were due to the debundling of the MWNTs.[17–19]

PS/MWNT nanocomposites having various compositions of MWNTs were fabricated. To elucidate the influence of end-functionalized polymers on nanocomposite properties, four kinds of matrices were applied: pure PS (M_w = 50,000 g/mol), pure PS–COOH (M_w = 50,000 g/mol), blends of PS (M_w = 50,000 g/mol) with 10 wt % PS–COOH (M_w = 3000 g/mol), and blends of PS (M_w = 50,000 g/mol) with 10 wt % PS–NH_2 (M_w = 3000 g/mol). Figure 3(A–C) shows optical photographs of MWNT nanocomposite films including 10 wt % MWNTs

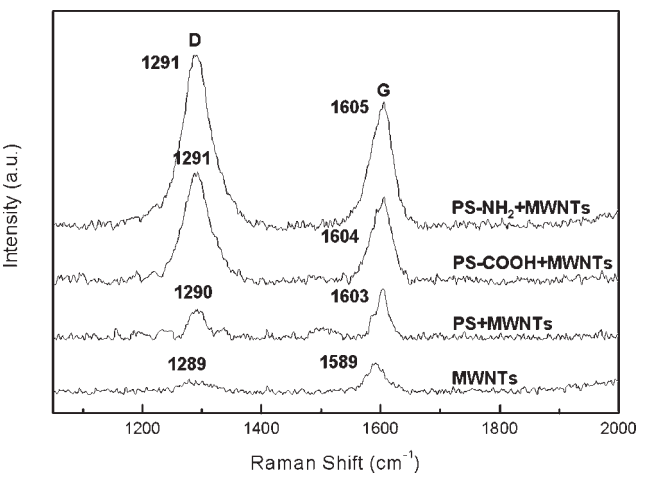

Figure 2 FT-Raman spectra of MWNTs and PS/MWNT nanocomposites. Pure MWNTs and nonfunctionalized PS/MWNT composites showed almost the same Raman spectra. In contrast, the high D/G band intensity ratios of the nanocomposites made from PS–COOH or PS–NH_2 indicated that the defect sites of MWNTs interacted sensitively with the end-functional groups of PS.

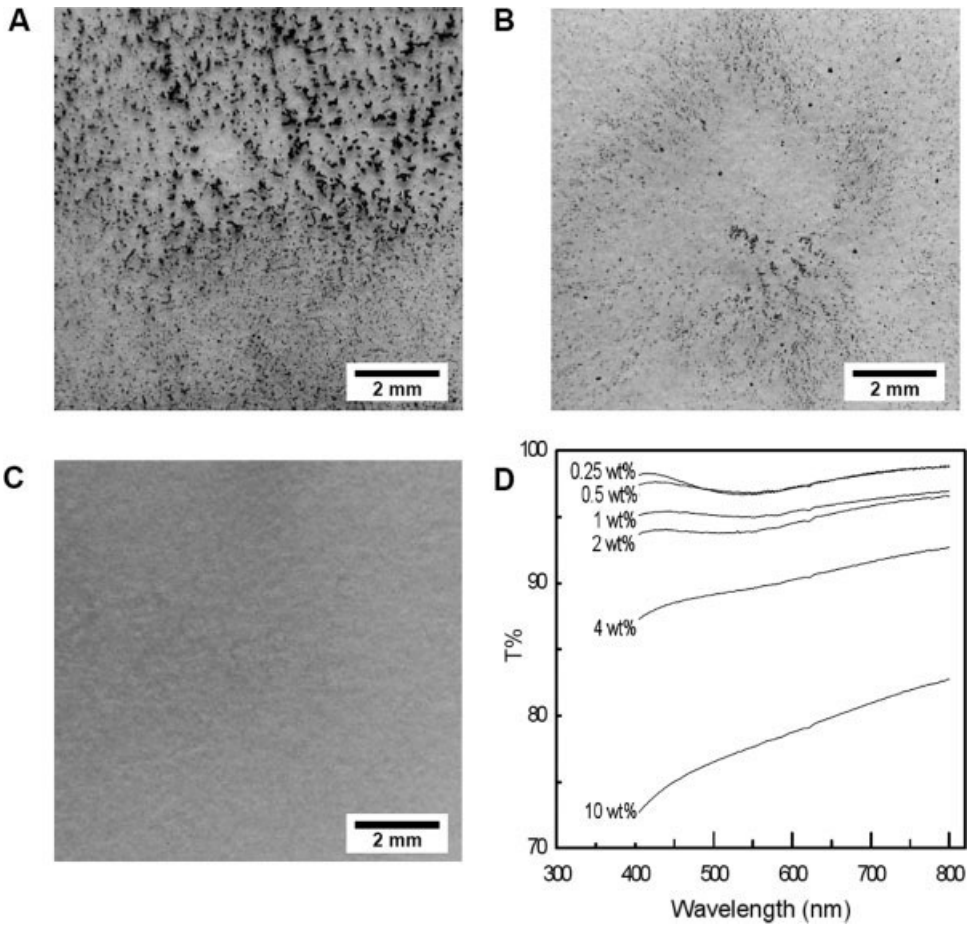

Figure 3 Optical micrographs of nanocomposite films including 10 wt % MWNTs in the matrix of (A) pure PS and blends of PS with (B) PS–COOH or (C) PS–NH_2 in a weight ratio of 9 : 1. (D) Optical transmittance of nanocomposite films including PS–NH_2 as a dispersant as a function of the MWNT concentration. The nanocomposites containing 4 wt % showed a high transmittance of approximately 90%. The film thickness was 120 nm.

prepared on glass substrates. The films, having a thickness of 120 nm, were prepared through the spin casting of a benzene solution dissolving both the polymer matrix and MWNTs. The dispersibility of MWNTs was remarkably influenced by the presence of end-functionalized polymers. MWNTs were hardly dispersed and aggregated in the film made from nonfunctionalized PS (M_w = 50,000 g/mol). By the addition of a small amount of end-functionalized polymers, the optical uniformity was greatly improved. Figure 3(B,C) shows the nanocomposite films including 10 wt % PS–COOH and PS–NH_2 (M_w = 3000 g/mol) in their matrices. MWNTs were well dispersed in the composites including PS–COOH, but small aggregates were still observed. By contrast, the nanocomposite film including PS–NH_2 dispersed MWNTs very well. The film was transparent throughout the film plane without any macroscopic aggregates. Figure 3(D) shows the optical transmittances of the nanocomposite films including 10 wt % PS–NH_2 in their matrices. The films incorporating less than 1 wt % MWNTs showed a very high transmittance of around 97–98% for all measured wavelengths. The films became turbid with the amount of MWNTs. However, the transmittance for the nanocomposites containing 4 wt % MWNTs kept a high value of approximately 90%.

To investigate the dispersion of MWNTs on a microscopic scale, SEM observations were performed for the fractured nanocomposite films including 5 wt % MWNTs [Fig. 4(A,B)]. The top surfaces of the films were weakly etched by RIE to expose the morphology of the MWNTs inside the matrix. As expected, a nonuniform dispersion of MWNTs was observed in the nanocomposites made from nonfunctionalized PS. A large aggregate of MWNTs having a diameter of over 30 μm is presented in Figure 4(A) as an inset. As shown in the magnified image of the cross section, MWNTs were pulled out of the matrix as a result of poor interfacial adhesion [Fig. 4(A)]. By contrast, the MWNTs were well dispersed and percolated in the nanocomposites including PS–NH_2 as a dispersant [Fig. 4(B)]. No large-size aggregate was found, and the film thickness was

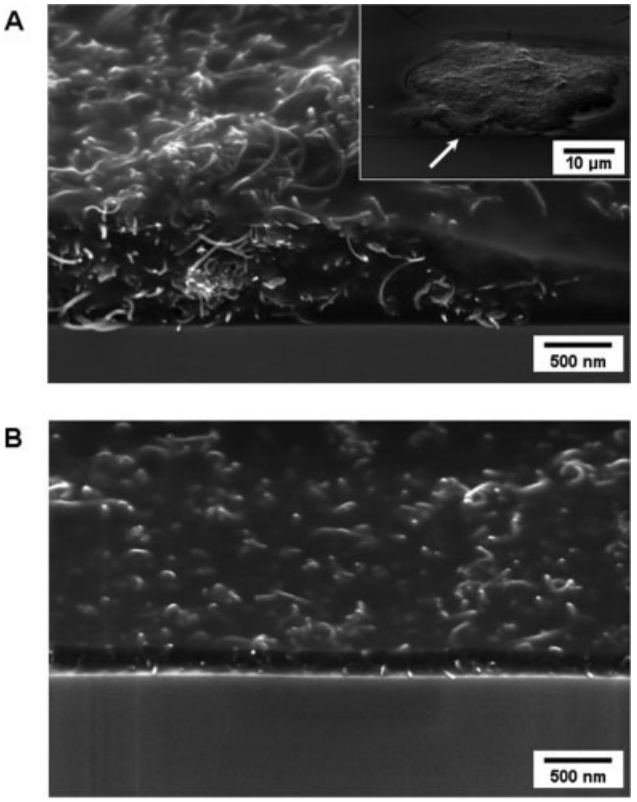

Figure 4 SEM images of 5 wt % MWNT nanocomposite films. The matrices were (A) PS and (B) blends of PS and PS–NH_2 in a weight ratio of 9 : 1. The inset in panel A is a low-magnification image of the pure PS/MWNT nanocomposite film. In panel A, a large aggregate of MWNTs can be observed. In contrast, the uniform dispersion and good interfacial adhesion of MWNTs are confirmed in panel B. The images were taken for samples that were tilted to 60°.

uniform. In the cross section, most MWNTs were broken at the fractured surface, and this indicated good interfacial adhesion. These SEM observations confirmed that end-functionalized polymers enhanced the interfacial adhesion as well as dispersibility of MWNTs in the polymer matrix.

The electrical and mechanical properties of various nanocomposites were characterized as a function of the MWNT concentration. Figure 5(A) shows the electrical resistivity of MWNT nanocomposite films against the weight fraction of MWNTs. The films containing PS–NH_2 demonstrated the lowest resistivity for all compositions. The resistivity at the percolation concentration was about 0.03 Ω m, which is suitable for electromagnetic interference shielding.[20,21]

Figure 5(B,C) shows the Young's modulus and hardness of PS/MWNT nanocomposite films. The mechanical properties were measured with a nanoindenter, a useful tool for thin films.[22,23] As expected, the nanocomposites including PS–NH_2 had the highest modulus and hardness values. Because of the fine dispersion of MWNTs, percolation occurred at a very low concentration of 0.4 wt %, at which the Young's modulus reached 8.7 GPa. It increased further to reach 13 GPa for a 10 wt % concentration of MWNTs, which corresponded to 3 times the modulus of a pure matrix film (4.5 GPa).

We assumed that the mechanical properties of the nanocomposites simply followed the rule of mixtures for fiber-reinforced composites by Krenchel:[24]

$$E_c = KE_fV_f + E_mV_m \tag{1}$$

where E_c, E_f, and E_m are the Young's moduli of the composite, fiber, and matrix, respectively; V_f and V_m are the volume fractions of the fiber and matrix, respectively; and K is the reinforcement efficiency, which is 3/8 in randomly oriented and uniformly distributed fiber-reinforced composites. The Young's modulus of the MWNTs was supposed to be about 1.28 GPa, and that of the PS matrix was measured to be 4.57 GPa.[25] The estimated Young's modulus was about 9.32 GPa for the composites including a 0.4 wt % concentration of MWNTs [Fig. 5(D)]. According to another widely used theory by Halpin and Tsai, the modulus of randomly oriented composites can be described as follows:

$$\frac{E_c}{E_m} = \frac{3}{8}\left[\frac{1+\zeta\eta_L V_f}{1-\eta_L V_f}\right] + \frac{5}{8}\left[\frac{1+2\eta_T V_f}{1-\eta_T V_f}\right] \tag{2}$$

where

$$\eta_L = \frac{E_f/E_m - 1}{E_f/E_m + \zeta} \tag{3}$$

$$\eta_T = \frac{E_f/E_m - 1}{E_f/E_m + 2} \tag{4}$$

$$\zeta = \frac{2L}{d} \tag{5}$$

MWNTs were assumed to be short fibers whose length (L) and diameter (d) were 5 μm and 20 nm, respectively. From this equation, the calculated modulus for 0.4 wt % MWNTs was 8.20 GPa.[26,27] These theoretical results were consistent with the experimental values for the nanocomposites including end-functionalized polymers, verifying that the well-dispersed MWNTs effectively reinforced the mechanical properties of the nanocomposites. The reinforcement by MWNTs could also be demonstrated in the hardness. Despite the presence of low-molecular-weight polymers, the nanocomposites including a small amount of end-functionalized polymers exhibited greater hardness than those made of single-component nonfunctionalized PS matrices. The nanocompo-

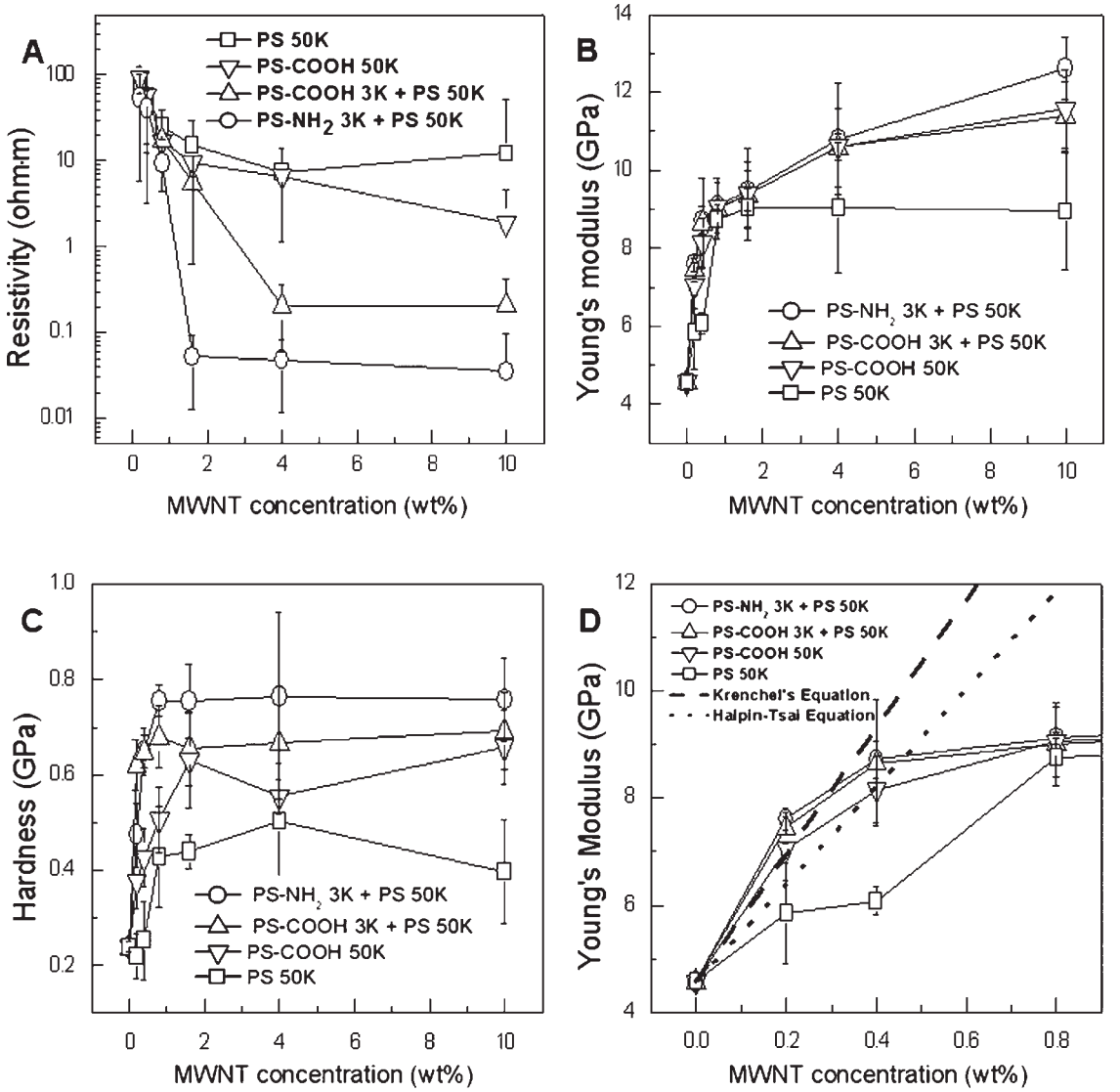

Figure 5 (A) Electrical resistivity, (B) Young's modulus, and (C) hardness of the PS/MWNT nanocomposite films. The nanocomposites including PS–NH_2 had the lowest electrical resistivity and the highest modulus and hardness values. (D) The theoretical and empirical Young's modulus of PS/MWNT nanocomposites. The empirical values for the composites including end-functionalized polymers agreed well with the theoretical values. Four kinds of matrices were used: PS (M_w = 50,000 g/mol), PS–COOH (M_w = 50,000 g/mol), a mixture of PS–NH_2 (M_w = 3000 g/mol) and PS (M_w = 50,000 g/mol), and a mixture of PS–COOH (M_w = 3000 g/mol) and PS (M_w = 50,000 g/mol).

sites made of a single-component matrix of a high-molecular-weight PS–COOH also showed improved mechanical properties. However, the improvement was limited, mainly because of the low density of the end-functional group.

CONCLUSIONS

A facile and highly effective strategy for preparing well-dispersed polymer/CNT nanocomposites has been introduced. The dispersibility of MWNTs in an organic solvent and polymer matrix was greatly improved in the presence of an end-functionalized polymer. The end-functionalized polymers were noncovalently grafted to MWNTs through hydrogen bonding or zwitterionic interactions, and this made them highly compatible with the surrounding organic media.[28–31] The finely dispersed state could be well preserved upon the fabrication of nanocomposite films having percolated structures. The physically grafted end-functionalized polymer also played an important role in improving the interfacial adhesion between the polymer matrices and MWNTs. The electrical and mechanical properties of PS/MWNT nanocomposite films were markedly improved through this noncovalent functionalization method.

References

1. Manchado, M. A. L.; Valentini, L.; Biagiotti, J.; Kenny, J. M. Carbon 2005, 43, 1499.
2. Thess, A.; Lee, R.; Nikolaev, P.; Dai, H.; Petit, P.; Robert, J.; Xu, C.; Lee, Y. H.; Kim, S. G.; Rinzler, A. G.; Colbert, D. T.; Scuseria, G. E.; Tomanek, D.; Fischer, J. E.; Smalley, R. E. Science 1996, 273, 483.
3. Cooper, C. A.; Cohen, S. R.; Barber, A. H.; Wagner, H. D. Appl Phys Lett 2002, 81, 3873.
4. Blond, D.; Barron, V.; Ruether, M.; Ryan, K. P.; Nicolosi, V.; Blau, W. J.; Coleman, J. N. Adv Funct Mater 2006, 16, 1608.
5. Coleman, J. N.; Cadek, M.; Blake, R.; Nicolosi, V.; Ryan, K. P.; Belton, C.; Fonseca, A.; Nagy, J. B.; Gun'ko, Y. K.; Blau, W. J. Adv Funct Mater 2004, 14, 791.
6. Chen, J.; Hamon, M. A.; Hu, H.; Chen, Y.; Rao, A. M.; Eklund, P. C.; Haddon, R. C. Science 1998, 282, 95.
7. Holzinger, M.; Vostrowsky, O.; Hirsch, A.; Hennrich, F.; Kapes, M.; Weiss, R.; Jellen, F. Angew Chem Int Ed 2001, 40, 4002.
8. Ham, H. T.; Koo, C. M.; Kim, S. O.; Choi, Y. S.; Chung, I. J. Macromol Res 2004, 12, 384.
9. Hirsch, A. Angew Chem Int Ed 2002, 41, 1853.
10. Lee, S. H.; Ham, H. T.; Park, J. S.; Chung, I. J.; Kim, S. O. Macromol Symp 2007, 249, 618.
11. Chen, R. J.; Zhang, Y.; Wang, D.; Dai, H. J Am Chem Soc 2006, 22, 8379.
12. Islam, M. F.; Rojas, E.; Bergey, D. M.; Johnson, A. T.; Yodh, A. G. Nano Lett 2003, 3, 269.
13. Kang, Y.; Taton, T. A. J Am Chem Soc 2003, 125, 5650.
14. Zheng, M.; Jagata, A.; Semke, E. D.; Diner, B. A.; Mclean, R. S.; Lustig, S. R.; Richardson, R. E.; Tassi, N. G. Nat Mater 2003, 2, 338.
15. Matsuura, K.; Saito, T.; Okazaki, T.; Ohshima, S.; Yumura, M.; Iijima, S. Chem Phys Lett 2006, 429, 497.
16. Dresselhaus, M. S.; Dresslhaus, G.; Saito, R.; Jorio, A. Phys Rep 2005, 409, 47.
17. Qin, S.; Qin, D.; Ford, W. T.; Herrera, J. E.; Resasco, D. E. Macromolecules 2004, 37, 9963.
18. Stephan, C.; Nguyen, T. P.; de la Chapelle, M. L.; Lefrant, S.; Journet, C.; Bernier, P. Synth Met 2000, 108, 139.
19. Rao, A. M.; Chen, J.; Richter, E.; Schlecht, U.; Eklund, P. C.; Haddon, R. C.; Venkateswaran, U. D.; Kwon, Y. K.; Tomanek, D. Phys Rev Lett 2001, 86, 3895.
20. Kim, H. M.; Kim, K.; Lee, C. Y.; Joo, J.; Cho, S. J.; Yoon, H. S.; Pejakovic, D. A.; Yoo, J. W.; Epstein, A. J. Appl Phys Lett 2004, 84, 589.
21. Ramasubramaniam, R.; Chen, J.; Liu, H. Appl Phys Lett 2003, 83, 2928.
22. Nix, W. D.; Medalist, R. F. M. Metall Trans A Phys Metall Mater Sci 1989, 20, 2217.
23. Bolshakov, A.; Oliver, W. C.; Pharr, G. M. J Mater Res 1996, 11, 760.
24. Krenchel, H. Fibre Reinforcement; Akademisk Forlag: Copenhagen, 1964.
25. Wong, E. W.; Sheehan, P. E.; Lieber, C. M. Science 1997, 277, 1971.
26. Halpin, J. C.; Kardos, J. L. Polym Eng Sci 1976, 16, 344.
27. Coleman, J. N.; Khan, U.; Blau, W. J.; Gun'ko, Y. K. Carbon 2006, 44, 1624.
28. Hamon, M. A.; Chen, J.; Hu, H.; Chen, Y.; Itkis, M. E.; Rao, A. M.; Eklund, P. C.; Haddon, R. C. Adv Mater 1999, 11, 824.
29. Chen, J.; Rao, A. M.; Lyuksyutov, S.; Itkis, M. E.; Hamon, M. A.; Hu, H.; Cohn, R. W.; Eklund, P. C.; Colbert, D. T.; Smalley, R. E.; Haddon, R. C. J Phys Chem B 2001, 105, 2525.
30. Kahn, M. G. C.; Banerjee, S.; Wong, S. S. Nano Lett 2002, 2, 1215.
31. Chattopadhyay, D.; Galeska, I.; Papadimitrakopoulos, F. J Am Chem Soc 2003, 125, 3370.